ical shift proximities and were taken at 500 MHz. Other experiments gave satisfactory results at 250 MHz. Gated decoupling used a 5-s saturating pulse. Following a 1-ms delay, a 6-ms rf pulse (55° tip angle) initiated the FID with an acquisition time of 1.7 s. A 10-s relaxation time followed before repetition of the pulse sequence. The data were processed by the method of spectral subtraction to enhance sensitivity. The results were obtained and are presented in the following form: proton saturated; proton signal(s) observed to be enhanced (% enhancement).

19: H_a; H_b (11), H_f (4), H_e (4). H_b; H_a (9), H_c (6). H_f; H_a (9), H_b (4), H_g (4).

20: H_a; H_b (4), H_f (17), H_e (7). H_b; H_a (3), H_f (7). H_f; H_a (11), H_b (10), H_e (2).

25: H_a; H_b (4), H_c (7), H_d (1), H_f (4). H_b; H_a (3), H_c (2), $H_f + H_b$ (2), H_g (2). H_c; H_a (3), H_b (3), H_d (4), $H_g + H_h$ (3).

28: H_a; $H_b + H_c$ (15) (possible enhancement of H_d not observed because of chemical shift proximity to H_a). $H_b + H_c$; H_a (13). H_d (500-MHz spectrum); H_a (11), H_h (3).

36: H_a; H_b (slight enhancement of ring proton signals). H_b; H_a (4), $H_c + H_d$ (11).

Pyrolysis of Chlorides 24 and 23. A sample of a **24/23** mixture (exo/endo = 8:1) in benzene-d_6 was heated at 55 °C for 3 h (100% conversion) and analyzed by 500-MHz ^{1}H NMR. The major product (>98%) was identified as benzyl chloride. At least 20 extraneous signals, corresponding to 1-2% of the total signal intensity, were present but not diagnostic. Further heating did not alter the spectrum. Identical results were obtained upon pyrolysis of a similar sample at lower temperature (35-50 °C) or upon partial pyrolysis in CD_3CN or in the gas phase.

Acknowledgment. We thank the National Science Foundation and the National Institutes of Health for support of this research.

Stereoelectronic Effects in Sulfate Diesters and Sulfuric Acid

Gordon Lowe,*,† Gregory R. J. Thatcher,†,‡ James C. G. Turner,§ Anne Waller,§ and David J. Watkin§

Contribution from The Dyson Perrins Laboratory, Oxford University, South Parks Road, Oxford OX1 3QY, England, and Chemical Crystallography, Oxford University, 9 Parks Road, Oxford OX1 3QS, England. *Received April 6, 1988*

Abstract: An X-ray crystallographic investigation of two 2,2-dioxo-1,3,2-dioxathianes has been undertaken, together with a comparative study of 1,1-dioxothiane, in a search for evidence of stereoelectronic effects in sulfate diesters. However, the differences between the axial and equatorial S=O bond lengths observed are so small that they cannot be detected by the X-ray experiment. Ab initio calculations on sulfuric acid and dimethyl sulfate showed that the sulfur–oxygen bond overlap populations, electron density at the sulfuryl oxygen atoms, and conformational energy were dependent on the S–OH(Me) torsion angle. These effects are interpreted in terms of stereoelectronic interactions between σ and π nonbonding electron pairs on divalent oxygen and the antibonding orbitals of sulfur–oxygen bonds. If an anomeric effect is defined simply as any $n \rightarrow \sigma^*$ orbital mixing interaction, this stereoelectronic effect must be viewed, at least in part, as anomeric. The stereoelectronic effect operating in H_2SO_4 and sulfate diesters may weaken S–O single bonds and influence overall charge distribution. Stereoelectronic effects in the chair conformation of six-membered cyclic sulfates result in the axial sulfuryl bond being longer than the equatorial. The bond length difference is such that it cannot be detected with confidence in the X-ray structure determinations presented, but it could account for the observed differences in the vibrational spectra of isotopically labeled sulfates.

The anomeric effect is widely recognized as having a major influence on the conformational preference of molecules containing geminal electronegative substituents.[1] Although this phenomenon was originally associated with sugars containing the RO–C–OH grouping it is not restricted to molecules with carbon as the central element, for example, 2-oxo-1,3,2-dioxathiane (**1**) adopts the chair conformation with the S=O axial.[2] If the underlying cause of the anomeric effect is stereoelectronic it would be expected that in 2,2-dioxo-1,3,2-dioxathiane (**2**) the axial S=O bond would be longer and the force constant weaker than that of the equatorial S=O bond. Indeed the differential isotope shift caused by heavy oxygen isotopes in the axial and equatorial S=O bonds of 2,2-dioxo-1,3,2-dioxathianes on the symmetric and antisymmetric SO_2 stretching frequencies provided support for this interpretation.[3]

We now report an X-ray crystallographic investigation of 2,2-dioxo-1,3,2-dioxathiane (**2**) and its 5-phenyl derivative (**3**) in order to explore the axial and equatorial S=O bond lengths. Since the equatorial S=O bond should not be susceptible to the generalized anomeric effect it should provide a valuable internal reference. A comparative X-ray crystallographic study of 1,1-dioxothiane (**4**) is also reported.

We have undertaken ab initio calculations with geometry optimization of a number of parameters simultaneously, including sulfur–oxygen bond lengths. This allows direct comparison with the crystal structures of **2** and **3**. In addition, conformation scans have been performed on H_2SO_4 corresponding to rotation about the S–O single bonds and bond angle changes at sulfur. All calculations include Mulliken population analysis. Bond overlap populations are the most widely used indicators for stereoelectronic effects (e.g., in calculations on P(V) species[4,5]) and provide an assessment of bond lengthening/shortening effects for conformers that are not fully geometry optimized. Calculations were also performed on rotamers of dimethyl sulfate.

In this study, the STO-3G* basis set is employed for conformational analysis and geometry optimization. Significant conformers are checked by geometry optimization and point calculations at the 3-21G(*) level. Limited calculations with a 4-31G

† The Dyson Perrins Laboratory, Oxford University.
‡ Present address: Queen's University, Kingston, Ontario, Canada.
§ Chemical Crystallography, Oxford University.

(1) (a) Kirby, A. J. *The Anomeric Effect and Related Stereoelectronic Effects at Oxygen*; Springer-Verlag: Berlin 1983. (b) Deslongchamps P. *Stereoelectronic Effects in Organic Chemistry*; Pergamon: Oxford, 1983. (c) Szarek, W. A.; Horton D., Eds. *The Anomeric Effect: Origin and Consequences*; American Chemical Society: Washington D.C., 1979; ACS Symp. Ser. 37. (d) Sinnott, M. L. *Adv. Phys. Org. Chem.* **1988**, 113.

(2) Altona, C.; Geise, H. J.; Romers, C. *Recl. Trav. Chim. Pays-Bas* **1966**, *85*, 1197.

(3) Lowe, G.; Parratt, M. J. *J. Chem. Soc., Chem. Commun.* **1985**, 1073; *Bioorg. Chem.* **1988**, *16*, 283.

(4) Lehn, J.-M.; Wipff, G. *J. Chem. Soc., Chem. Commun.* **1975**, 800.

(5) Gorenstein, D. G.; Luxon, B. A.; Findlay, J. B. *J. Am. Chem. Soc.* **1979**, *101*, 5869 and references cited therein.

0002-7863/88/1510-8512$01.50/0

and minimal STO-3G basis set provide useful comparisons between these different levels of calculation.

Materials and Methods

Melting points were recorded on a Reichert apparatus and are uncorrected. Infrared spectra were recorded on a Perkin-Elmer FTIR 1750 spectrophotometer. Mass spectra in the electron impact mode were recorded on a VG Micromass 16F spectrometer.

2,2-Dioxo-1,3,2-dioxathiane (2) (with C. E. Haines). 2-Oxo-1,3,2-dioxathiane[6] was oxidized with ruthenium tetroxide[7] to give 2,2-dioxo-1,3,2-dioxathiane as needles from ether, mp 60 °C (lit.[8,9] mp 62 and 63 °C).

2,2-Dioxo-5-phenyl-1,3,2-dioxathiane (3). 2-Oxo-5-phenyl-1,3,2-dioxathiane was oxidized with ruthenium tetroxide[10] to give **3** as needles from ether (mp 84.5–85.5 °C): mass spectrum (EI), *m/e* 214; FTIR (CCl_4), ν_{max} (S=O antisym) 1418 cm^{-1}, ν_{max} (S=O sym) 1230 cm^{-1}.

1,1-Dioxothiane (4) (with C. E. Haines). 1-Oxothiane was prepared from pentamethylene sulfide[11,12] and oxidized with ruthenium tetroxide[7] to give 1,1-dioxothiane, which after crystallization from ether had mp 97 °C (lit.[13] mp 98.5–99 °C).

X-ray Crystallography. The X-ray diffraction intensity data were collected on the CAD4-F diffractometer and the structures solved and refined with the CRYSTALS program, unless otherwise stated.

(i) 2,2-Dioxo-1,3,2-dioxathiane (**2**), $C_3H_6O_4S$, M_r = 138.14. Crystal data: monoclinic, space group $P2_1/n$; a = 6.264 (1) Å, b = 10.479 (2) Å, c = 8.552 (3) Å; β = 96.74 (2)°; V = 557.47 Å^3; Z = 4, ρ = 1.65 mg m^{-3} Mo radiation λ = 0.71069 Å; μ = 4.80 cm^{-1}.

A prescan produced an orientation matrix and accurate cell dimensions. A total of 2813 reflections were collected between 0 and 32° in θ. Data reduction produced 1948 independent reflections, 1183 of which were used in the subsequent refinement.

The structure was solved with MULTAN[14] and refined with CRYSTALS[15] by full-matrix least squares, first with isotropic and then anisotropic temperature factors. Corrections were made for secondary extinction and anomalous dispersion effects. For the final cycle of refinement a weighting scheme was introduced. The necessary weights were calculated from a truncated Chebychev polynomial. The refinement converged at a final value of R = 3.34%.

(ii) 2,2-Dioxo-5-phenyl-1,3,2-dioxathiane (**3**), $C_9H_{10}O_4S$, M_r = 214.24. Crystal data: space group $P2_1/a$; a = 8.941 (2) Å, b = 16.300 (1) Å, c = 6.903 (1) Å; β = 92.552 (14)°; V = 1005.11 Å^3; Z = 4; ρ = 1.42 mg m^{-3}; Cu Kα radiation λ = 1.5418 Å; μ = 27.3 cm^{-1}.

The reflections were corrected for absorption, although the effect on the data was minimal. The maximum absorption correction applied was 1.19. The structure was solved with the direct methods program SHELXS[16] and refined with CRYSTALS. All non-hydrogen atoms were located and refined with respect to their positional and anisotropic temperature factors. The hydrogens were added by the geometrical placing routine, although most of the hydrogens could be discerned from a difference Fourier map. The hydrogen parameters were not refined. The structure was then corrected to take secondary extinction and anomalous dispersion into account and refined to convergence with unit weights. The refinement converged at a final value of R = 4.28%.

(iii) 1,1-Dioxothiane (**4**), $C_5H_{10}O_2S$, M_r = 134.19. Crystal data: monoclinic, space group $P2_1/a$; a = 8.385 (3) Å, b = 8.945 (4) Å, c = 8.980 (3) Å, β = 101.64 (3)°; V = 659.92 Å^3; Z = 4; ρ = 1.35 mg m^{-3} cm^{-1}; Mo radiation λ = 0.71069 Å; μ = 3.84 cm^{-1}.

A prescan produced an orientation matrix and accurate cell density. A total of 1053 reflections were collected between 0 and 20° in θ. After data reduction there were 574 independent reflections of which 537 were used for refinements.

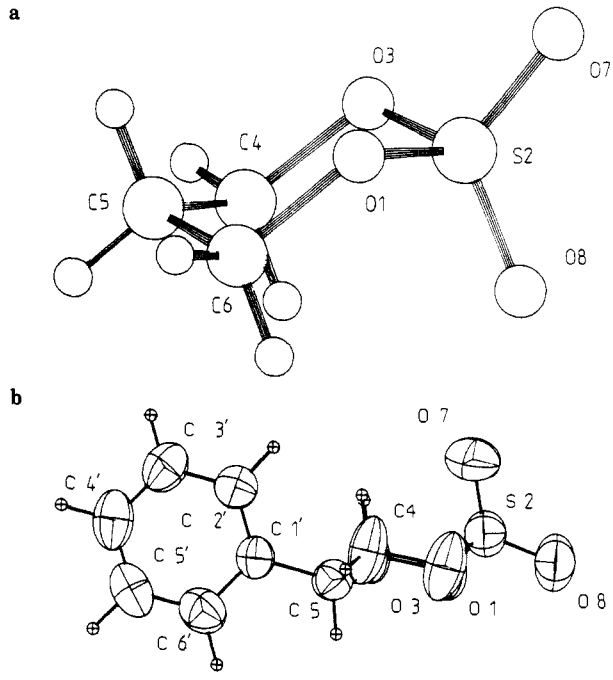

Figure 1. (a) Stereochemical representation of 2,2-dioxo-1,3,2-dioxathiane (**2**) and (b) thermal ellipsoid representation of 2,2-dioxo-5-phenyl-1,3,2-dioxathiane (**3**) from X-ray crystal structure analysis.

Table I. Bond Lengths (Å) and Angles from X-ray Crystal Structure Analysis of Sulfates **2** and **3**, Sulfone **4**, and Sulfite **1**

	2	**3**[a]	**3**[b]	**4**	**1**[c]
d(S=O_{ax})	1.415 (2)	1.402 (3)	1.444	1.439 (3)	1.45 (1)
d(S=O_{eq})	1.413 (2)	1.415 (3)	1.430	1.447 (2)	
d(S—$O_3(C_2)$)	1.551 (2)	1.538 (3)	1.580	1.756 (4)	1.46 (1)
d(S—$O_1(C_6)$)	1.552 (2)	1.540 (3)	1.579	1.759 (4)	1.46 (1)
∠O–S–O	119.5 (1)	121.5 (2)	121.5	116.9 (2)	
∠O(C)–S–O(C)	102.6 (1)	101.3 (2)	101.3	109.5 (1)	

[a] Uncorrected bond lengths. [b] Bond lengths corrected for libration from thermal parameters. [c] Reference 2.

The structure was solved with MITHRIL[17] and refined with CRYSTALS by full-matrix least squares, first with isotropic and then anisotropic temperature factors. Corrections were made for secondary extinction and anomalous dispersion effects. For the final cycle of refinement a weighting scheme was introduced. The necessary weights were calculated from a truncated Chebychev polynomial. The refinement converged at a final value of R = 3.18%.

MO Calculations Method. H_2SO_4 is expected to be a better model than dimethyl sulfate for detection of stereoelectronic effects, since steric interactions involving the bulkier methyl groups of dimethyl sulfate may obscure weaker stereoelectronic effects in this system. O–H bond lengths and S–O–H bond angles were constrained at 0.97 Å and 108.5°, respectively. S–O–C bond angles and O–C and C–H bond lengths were constrained at 114.5°, 1.478 Å, and 1.0 Å. The latter values were derived from the crystal structures of cyclic sulfates **2** and **3**. The angle between the O—S—O and O=S=O planes (τ) was maintained at 90°. The experimentally observed value for H_2SO_4 is 88.4°.[18] O—S=O bond angles were constrained to be equivalent. Sulfur–oxygen single bonds were generally constrained to be equal. Calculations were performed at the RHF/3-21G(*),[19a] RHF/4-31G,[19b] RHF/STO-3G*,[19c] and RHF/STO-3G[19d] levels with the program GAUSSIAN 82.[19e] Geometry optimization within these programs employs the Schlaeger gradient optimization algorithm.

(6) Van Woerden, H. F.; Havinga, F. *Recl. Trav. Chim. Pays-Bas* **1967**, *86*, 353.
(7) Lowe, G.; Salamone, S. J. *J. Chem. Soc., Chem. Commun.* **1983**, 1392.
(8) Kaiser, E. T.; Panar, M.; Westheimer, F. H. *J. Am. Chem. Soc.* **1963**, 85, 602.
(9) Carlson, W. W.; Cretcher, L. H. *J. Am. Chem. Soc.* **1947**, *69*, 1952.
(10) Lowe, G.; Parratt, M. J.; Salamone, S.; Thatcher, G. R. J., in preparation.
(11) Chadka, V. K.; Leidel, K. G.; Plapp, B. V. *J. Med. Chem.* **1983**, *26*, 916.
(12) Leonard, N. J.; Johnson, C. R. *J. Org. Chem.* **1962**, *27*, 282.
(13) Grishkevitch-Trokhimovskii, E. *J. Russ. Phys. Chem. Soc.* **1916**, *48*, 928; *Chem. Abstr.* **1917**, *11*, 786.
(14) Main, P., et al., MULTAN 80, a system of computer programs for the automatic solution of crystal structures from X-ray data, Department of Physics, University of York, 1980.
(15) Watkins, D. J.; Carruthers, J. R.; Betheridge, P. W. *Crystals User Guide*; Chemical Crystallography Lab.: Oxford, 1985.
(16) Sheldrich, G. M. In *Crystallographic Computing*; Sheldrich, G. M., et al., Eds.; Oxford University Press, 1985.
(17) Gilmore, MITHRIL, a computer program for the automatic solution of crystal structures from X-ray data, Department of Chemistry, University of Glasgow, 1983.
(18) Kuczowski, R. L.; Suenram, R. D.; Lovas, F. J. *J. Am. Chem. Soc.* **1981**, *103*, 2561.
(19) (a) Pietro, W. J.; Francl, M. M.; Hehre, W. J.; DeFrees, D. J.; Pople, J. A.; Binkley, J. S. *J. Am. Chem. Soc.* **1982**, *104*, 5039. (b) Hehre, W. J.; Lathan, W. A. *J. Chem. Phys.* **1972**, *56*, 5225. (c) Collins, J. B.; Schleyer, P. v. R.; Binkley, J. S.; Pople, J. A. *J. Chem. Phys.* **1976**, *64*, 5142. (d) Hehre, W. J.; Stewart, R. F.; Pople, J. A. *J. Chem. Phys.* **1969**, *51*, 2567. (e) Frisch, M., Gaussian 82 Revision H. Version, Carnegie-Mellon University, 1985.

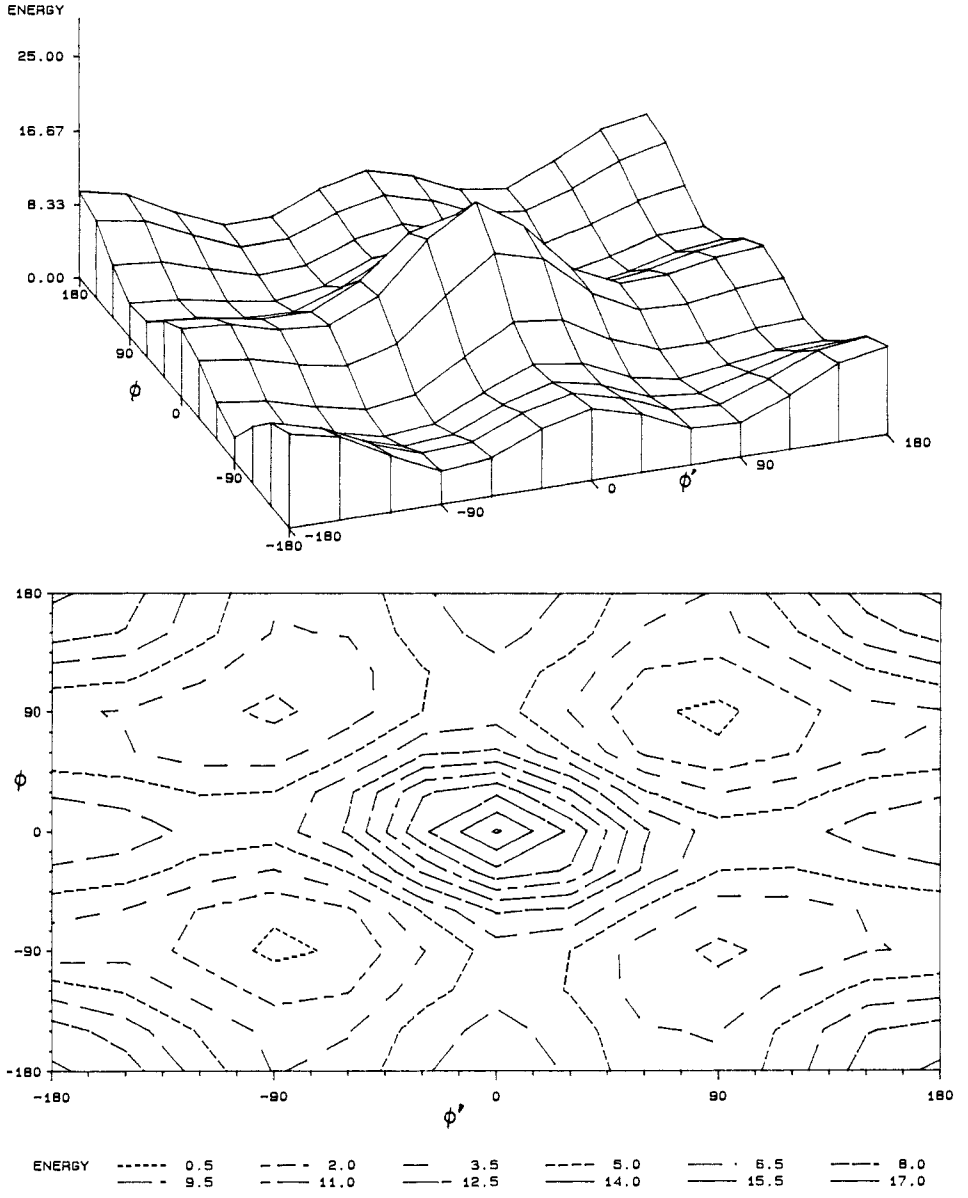

Figure 2. Conformational energy (kcal/mol) of H_2SO_4 as a function of torsion angles (ϕ,ϕ') about S–O single bonds, calculated at the STO-3G(*) level: (a) 3-D representation; (b) energy contour map.

Results

X-ray Crystal Structure Analysis. The structures of 2,2-dioxo-1,3,2-dioxathiane (**2**) and 5-phenyl-2,2-dioxo-1,3,2-dioxathiane (**3**) (Figure 1) and 1,1-dioxothiane (**4**) were determined. Significant bond lengths and angles from these analyses are given in Table I. The thermal parameters for **3** were indicative of librational motion centered at the sulfate moiety. The presence of significant correlated libration was confirmed by a TLS calculation[20] on the thermal parameters of **3**, in which the SO_4 fragment was treated as a rigid body (bond angles constrained). Bond lengths corrected for this libration are given in Table I. Similar results were obtained with the inclusion of C_4 and C_6 in the rigid body.

Molecular Orbital Calculation Analysis. Conformational Analysis: Torsion Angle Variation. Geometry optimization of H_2SO_4 at the STO-3G* level was employed to obtain a basis structure for conformational analysis. Optimization of (i) S=O and S—O bond lengths (S—O bonds constrained equal), (ii) O—S—O and O=S=O bond angles, and (iii) HO–SO torsional angles yielded the +sc, +sc conformation (82.5°,82.5°) (see Table II) as the minimum energy conformer. The torsional angles were varied in increments of 30° (Chart I). Molecular energy and Mulliken population were calculated at each point. With these data and the geometric equivalence inherent in the tetrahedral structure, the conformational energy and S–O_6 bond overlap population may be obtained as a function of the torsional conformational angle.

Chart I

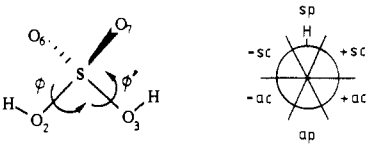

The potential energy surface corresponding to rotation about the S–O single bonds of H_2SO_4 has a global maximum at 0°,0° (sp,sp) and a global minimum at 90°,90° (+sc,+sc) (and the mirror –sc,–sc conformation) (Figure 2). The +sc,–sc conformation (90°,–90°) (and mirror –sc,+sc conformer) represents a local minimum. The ap,ap conformation (180°,180°) is a local maximum. The possibility that the +sc,–sc conformation is the global minimum is addressed through geometry optimization of this conformation, which confirms this conformer (89.9°,–89.9°) to be a true local minimum, 1.7 kcal/mol higher in energy than

(20) Johnson, C. K. *Crystallographic Computing*; Ahmed, F. R., Ed.; Munksgaard, 1970.

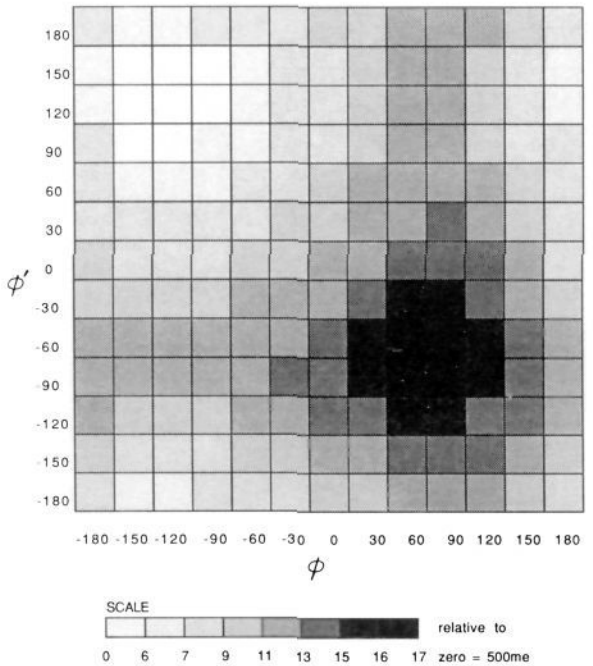

Figure 3. S=O_6 bond overlap population (millielectrons) as a function of torsion angles (ϕ,ϕ') about S—O single bonds, from Mulliken population analysis of H_2SO_4 at the STO-3G(*) level.

the global minimum. Geometry optimization of the sp,sp (0°,0°) energy maximum and the ap,ap (180°,180°) local maximum leads to a reduction in conformational energy of 1.4 and 5.5 kcal/mol, respectively (Table II).

Geometry optimization of the minimum energy conformers of H_2SO_4 at the 3-21G(*) level shows the absolute minimum to be the +ac,+ac (100°, 100°) conformation (Table II). The +sc,–sc local minimum (90°,–90°) is 2.1 kcal/mol higher in energy than the absolute minimum at the 3-21G(*) level (cf. 1.7 kcal/mol at the STO-3G(*) level).

The overlap populations for one S=O double bond as a function of torsion angle are plotted in Figure 3. This plot depicts changes in sulfuryl bond order as both S–O single bonds are rotated through 360°. It can be seen that the regions of maximum and minimum overlap population coincide with +sc,–sc and –ac,+ac conformations, respectively. Changes in overlap population are minimized in the remaining two quadrants.

Two sections through this electron density surface are drawn in Figure 4c and are compared with changes in S–O single bond overlap population and charge density at sulfuryl oxygen as a function of torsion angle (Figure 4, parts a and b). For reference, the scale of each abscissa is equal to the maximum variation in each property plotted over the total conformational surface. Charge density at sulfuryl oxygen is the most responsive parameter to conformational change. An inverse relationship exists between S=O double bond overlap population and charge at sulfuryl oxygen. Overlap populations indicate that S—O single bond weakening occurs when the bond is sp ($\phi' = 0°$) to the hydrogen of the adjacent hydroxy substituent, regardless of torsional angle. Conversely, S=O double bond weakening is concomitant with an ac interaction with one S—OH substituent, again independent of the second torsional angle. Although only two torsional cross sections are plotted ($\phi' = 0°$, 180°), these trends apply across the entire conformational surface.

If overlap population is used as an indicator of bond order and bond length, then differences between S=O bond overlap populations qualitatively estimate differences between S=O double bond lengths. The largest difference (centered on 90°,–90°) is observed for conformations with one S–O bond +ac or +sc and the second –ac or –sc.

Conformational Analysis: Bond Angle Variation. A limited conformational scan was made of bond angle distortion. Bond

Table II. Geometry Optimized Parameters for H_2SO_4 Calculated at the STO-3G* and 3-21G(*) Levels, (Comparison with Experimentally Determined Geometrical Parameters)

structure method	H_2SO_4 micro- wave[a]	2 X-ray	3 X-ray	H_2SO_4 STO- 13G*[b]	H_2SO_4 STO- 3G*[b]	H_2SO_4 STO- 3G*	H_2SO_4 STO- 3G*	H_2SO_4 STO- 3G*[b]	H_2SO_4 3-21G(*)[b]	H_2SO_4 3-21G(*)[b]	H_2SO_4 3-21G(*)[b]	H_2SO_4 3-21G(*)[b]	H_2SO_4 3-21G(*)[b]
ϕ	90.9	60.1		60	82.5	0	180	89.9	60	100.2	114.9	180	0
ϕ'	–90.9	–59.8		–60	82.5	0	180	–89.9	–60	100.2	–114.9	180	0
d(S=O_{ax})[d]	1.422 (10)	1.402	1.415	1.450	1.447	1.447	1.450	1.452	1.418	1.415	1.423	1.419	1.411
d(S=Oeq)		1.415	1.413	1.442	1.447	1.447	1.450	1.442	1.405	1.415	1.410	1.419	1.411
d(S—O_{ax})	1.574 (10)	1.539[e]	1.552[e]	1.621	1.615	1.615	1.638	1.616	1.583	1.571	1.572	1.568	1.604
Δd(S=O)		0.005	0.002	0.008	0	0	0	0	0.013	0	0.013	0	0
∠O=S=O	123.3 (10)	121.5	119.5	125.0	125.6	125.6	122.9	121.3	125.7	123.5	122.9	122.2	119.0	122.2
∠O—S—O	101.3 (10)	101.3	102.6	101.4	100.3	100.3	102.7	89.7	100.6	101.4	101.3	101.0	95.3	101.7
E(rel)[f]				4.5	0	0	15.8	4.3	1.7	9.0	0	2.2	3.1	21.2
OP(S=O_{ax})[g]				0.5054	0.5123	0.5123	0.5110	0.5038	0.5026	0.5181	0.5215	0.4937	0.5236	0.5346
OP(S=O_{eq})				0.5210	0.5123	0.5123	0.5110	0.5038	0.5208	0.5391	0.5215	0.5448	0.5236	0.5346
OP(S—O_{av})				0.3227	0.3276	0.3276	0.3093	0.3283	0.3275	0.2321	0.2533	0.2535	0.2544	0.2227

[a] Reference 14. [b] S–O bonds constrained equal. [c] Nonoptimized parameter. [d] Bond lengths (Å) for exocyclic (pseudo)axial and (pseudo)equatorial and endocyclic sulfur–oxygen bonds. [e] Bond lengths averaged. [f] Conformational energy (kcal/mol) relative to minimum for basis set employed. [g] Bond overlap populations (electrons), from Mulliken population analysis.

Table III. Geometrical Parameters for H_2SO_4 and Dimethyl Sulfate for Conformers Mimicking Six-Membered Cyclic (60°,-60°) Sulfates. Partial Geometry Optimization and Comparison of Basis Sets

structure	Me_2SO_4	H_2SO_4	H_2SO_4	H_2SO_4	H_2SO_4	H_2SO_4	H_2SO_4	Me_2SO_4
method or basis set	e⁻ diffraction[a]	STO-3G	STO-3G(*)	STO-3G(*)	STO-3G(*)	3-21G(*)	4-31G	STO-3G(*)
ϕ, ϕ'	180, 180	60, -60	60, 60	60, -60	60, -60	60, -60	60, -60	60, -60
$d(S{=}O_{ax})$[b]	1.419	1.827[g]	1.447[g]	1.451[g]	1.452[g]	1.418[g]	1.572[g]	1.454[g]
$d(S{=}O_{eq})$[b]	1.419	1.742[g]	1.447[g]	1.443[g]	1.443[g]	1.405[g]	1.565[g]	1.445[g]
$d(S{-}O_{end})$[b]	1.567	1.567	1.567	1.567	1.574	1.567	1.567	1.539
Δd(exo)[c]		0.085	0	0.008	0.009	0.013	0.007	0.009
∠O=S=O	122.3	122.4	122.4	122.4	120.4	122.4	122.4	120.4
∠O—S—O	96.72	96.72	96.72	96.72	101.3	96.72	96.72	101.3
∠H—C—O								113.8[g]
E(rel)[d]			5.6	9.5	7.4	10.5		
$OP(S{=}O_{ax})$[e]		0.0552	0.5133	0.5064	0.5059	0.5233	0.1683	0.5061
$OP(S{=}O_{eq})$[e]		0.0781	0.5133	0.5205	0.5201	0.5421	0.1832	0.5193
$OP(S{-}O_{end})$[e]		0.1558	0.3450	0.3443	0.3411	0.2315	-0.0979	0.3535

[a] Reference 25. [b] Bond lengths (Å) of pseudoaxial and pseudoequatorial S=O bonds and pseudo-endocyclic S—O bonds. [c] Difference between exocyclic S=O bond lengths. [d] Conformational energy (kcal/mol) relative to minimum energy conformation for each basis set. [e] Bond overlap population (electrons). [g] Geometry optimized parameters.

lengths identical with those used for the torsion angle scan were employed. The O—S—O and O=S=O bond angles of the +sc,-sc conformer (60°,-60°) were varied in six steps between 88.0° and 105.0° and in five steps between 120.8° and 126.0°, respectively. A Mulliken population analysis and conformational energy calculation was performed at each point. Bond angle distortion for the +sc,-sc conformation has a minimal effect on electron distribution over the sulfuryl bonds. Overlap populations of the pseudoequatorial and pseudoaxial S=O double bonds vary by 3.6 and 2.0 me, respectively. The maximum variation in S—O single bond overlap population is 1.2 me.

Geometry Optimized Structures: 1. Bond Length Differences. The difference in bond length between the two S=O double bonds ranges from 0 to 0.013 Å (Tables II and III). No difference in bond length is observed for +sc,+sc and +ac,+ac conformations, in which the sulfuryl bonds are equivalent. The +sc,-sc conformers (60°,-60°) model the six-membered cyclic sulfates in which one S=O bond is pseudoaxial and the second pseudoequatorial. The STO-3G minimal basis set gives a difference in bond lengths of 0.085 Å between these two S=O bonds, the pseudoaxial being the longer. This difference is much smaller at the higher levels of calculation, ranging from 0.008 to 0.013 Å. The value for the +sc,-sc (90°,-90°) conformation lies within this range. The results of calculations on H_2SO_4 are confirmed by calculations on dimethyl sulfate.

2. Comparison between Basis Sets and Experiment. The data for partially optimized structures (Table III) include optimized S=O double bond lengths calculated with various basis sets. It can be seen from inspection of Tables II and III that all calculated bond lengths are overestimated relative to experimental values, with the exception of calculations at the 3-21G(*) level. Mean calculated S=O bond lengths are greater than the experimental mean for dimethyl sulfate and H_2SO_4 (1.4205 Å) by 0.364, 0.161, and 0.027 Å at the STO-3G, 4-31G, and STO-3G* levels, respectively. At the STO-3G* level, very little change is detected in the values of S=O double bond lengths, when: (i) the mean geometry of cyclic sulfates **2** and **3** is employed, (ii) calculation is performed on dimethyl sulfate, and (iii) the symmetrical +sc,+sc (60°,60°) conformation is used (Tables III and IV). At the 3-21G(*)level optimized bond lengths and angles of +sc,+sc and +sc,-sc conformations are well within the experimental error limits of the microwave geometry of H_2SO_4.

Consideration of the Δd(S=O) values obtained at the minimal STO-3G level (Table III) suggests that calculations on H_2SO_4 at this level must be viewed with circumspection. Geometrical and Mulliken population parameters obtained at the 4-31G level also indicate that this basis set is not ideal for the study of sulfates.

3. Bond Angles at Sulfur. Optimized geometries show considerable variation in bond angles at the STO-3G* level. The O=S=O bond angle varies by 4.3° and the O—S—O bond angle by 13.0° (Table II). The smallest bond angles are found for the ap,ap conformation, the largest O=S=O bond angle for the +sc,+sc conformation, and the widest O—S—O bond angle for the sp,sp conformer. A somewhat similar set of values was ob-

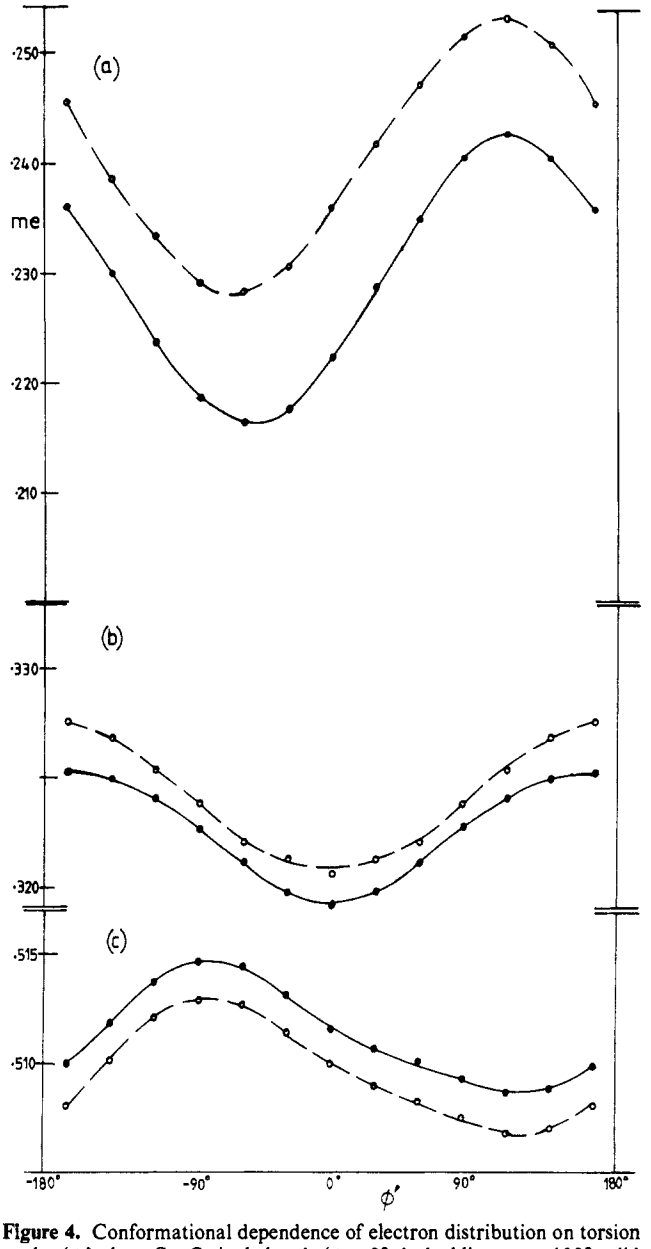

Figure 4. Conformational dependence of electron distribution on torsion angles (ϕ') about S—O single bonds (ϕ = 0° dashed lines, ϕ = 180° solid lines) from Mulliken population analysis of H_2SO_4 at the STO-3G(*) level: (a) charge at O_6; (b) S—O_2 bond overlap population; (c) S=O_6 bond overlap population.

Table IV. Structural Parameters for Dimethyl Sulfate Geometry Optimized at the STO-3G* Level[a]

	conformer					
	+sc,+sc	sp,+ac	ap,ap	+ac,-ac	ap,+sc	+sc,-sc
ϕ	72.5	0*	180*	120*	180*	72.5*
ϕ'	72.5	102.7	180*	-120*	72.6	-72.5*
$d(S{=}O_6)$	1.447	1.446	1.450	1.451	1.446	1.452
$d(S{=}O_7)$	1.447	1.449	1.450	1.445	1.451	1.442
d(S—O endo)	1.620	1.632	1.620	1.626	1.619	1.630
∠O=S=O	124.6	123.6	121.4	123.9	122.9	125.2
∠O—S—O	100.4	102.4	88.8	96.1	94.7	106.8
Δd(S=O)	0	0.003	0	0.006	0.005	0.01
E(rel)[b]	0	8.2	3.8	5.4	1.7	7.5

[a] Nonoptimized parameters are marked with an asterisk. [b] Energy (kcal/mol) relative to minimum energy +sc,+sc conformation.

served by Kaliannan et al.,[21] although the present data do not support a suggested direct correlation between increasing O—S—O and O=S=O bond angle with increasing conformational torsion angle size.[21] In addition, the trends in relative conformational bond angles are not followed at the higher 3-21G(*) level. Calculations at the STO-3G* level appear to substantially overestimate these conformationally dependent bond angle changes. Calculated bond angles at the 3-21G(*) level vary little from experimentally determined values.

4. Choice of Model. The similarity between data from calculations on H_2SO_4 and dimethyl sulfate confirms that H_2SO_4 is a valid model for cyclic and acyclic sulfate diesters, for the purpose of this study (Tables II and IV). The results of more comprehensive geometry optimizations also confirm that for calculations on symmetrical species (i.e., $\phi = \pm\phi'$) the equivalence of the single bonds is an acceptable constraint and does not interfere with energy minimization (Table II).

Discussion

Crystal Structure Analysis. All three six-membered heterocycles adopt the chair conformation, with one exocyclic oxygen axial and the second in an equatorial orientation. The exocyclic sulfuryl bond lengths approach values for "pure" double bonds, whereas endocyclic S–O bond lengths conform to bond orders of ca. 1.3.[22] This suggests the involvement of sulfur d-orbitals in p → dπ bonding interactions with nonbonding electrons on oxygen. Similar effects are observed in phosphorus chemistry.[23] The sulfuryl bond lengths of the sulfone are slightly longer than those of the sulfates, reflecting the lower electronegativity of the endocyclic carbon substituents of the sulfone relative to the endocyclic oxygens of the sulfate.

Trimethylene sulfite **1** provides a direct comparison with cyclic sulfate **2**. Both S—O single and double bonds are longer in the sulfite structure, reflecting the increased electronegativity and inductive effect of the second sulfuryl oxygen of the sulfate. The geometry of dimethyl sulfate derived from electron diffraction data[24] and the structure of sulfuric acid determined by microwave spectroscopy[21] are given in Tables III and II, respectively.

Gillespie and Robinson have formulated empirical relationships between S=O stretching frequency and (i) O=S=O bond angle and (ii) S=O bond length.[22] The crystallographic data and observed stretching frequencies for **2** and **3** conform to these relationships.

The Generalized Anomeric Effect. The generalized anomeric effect has been discussed in detail.[1] Effects on bond lengths and bond angles are attributed to the anomeric effect: (i) polar bonds antiperiplanar (app) to a lone pair are lengthened relative to those possessing no app interaction and (ii) bond angles are increased

Chart II

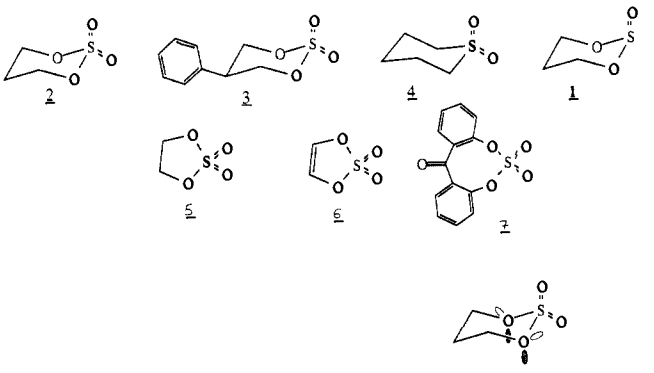

at anomeric centers in the presence of an app interaction. Anomeric bond lengthening of 0.04 Å has been proposed for exocyclic C–Cl bonds.[25] In pyranose derivatives, anomeric bond lengthening is ≤0.02 Å.[1a] Two recent studies have catalogued structural data for a large sample of species in which the anomeric effect is manifest.[26,27]

Sulfates and Phosphates. The ab initio calculations of Lehn and Wipff on H_3PO_4 and trimethyl phosphate indicated the presence of an anomeric effect.[4] Subsequent calculations indicated an anomeric bond lengthening effect: phosphorus–oxygen single and double bond lengths varying by ≤0.003 and ≤0.001 Å, respectively.[28] Lehn and Wipff predicted that similar stereoelectronic effects would be observed in other systems, including sulfates.

Structural Analysis. In the chair form, six-membered cyclic sulfates are locked in a +sc,-sc conformation (60°,-60°) with respect to the torsional angles about the endocyclic S—O bonds. In this conformation, the axial exocyclic S=O bond is subject to two antiperiplanar lone pair interactions (Chart II). Since the torsional and bond angles at the anomeric center (sulfur) are controlled by the constraints of the ring, the sulfuryl bond lengths themselves are the only indication of an anomeric effect. X-ray analysis shows the axial S=O bond to be 0.002 Å longer than the equatorial S=O bond in sulfate **2**, 0.013 Å shorter in sulfate **3**, and 0.014 Å longer in sulfate **3** when corrected for libration (Table I). Axial bond lengthening is predicted by the generalized anomeric effect. However, the bond lengths are only reliable with a 99% probability within three standard deviations and hence the axial and equatorial bond lengths for sulfates **2** and **3** cannot be said to differ. The axial sulfuryl bond of sulfone **4**, which serves as a nonanomeric control, is shorter than the equatorial S=O bond by 0.008 Å. However, when the sulfone S=O double bond lengths are fixed as nearly identical (through programmable constraints: $S{=}O_{ax}$ = 1.441 (3) Å; $S{=}O_{eq}$ = 1.446 (3) Å), refinement of the crystal data yields an unchanged R value of 3.18%.

The estimated errors involved in crystal structure analyses of **2**, **3**, and **4** are too great to allow any deductions to be made about the generalized anomeric effect. If an anomeric effect does apply to these systems its influence on S=O double bond length must be small. It would, however, be useful to estimate the expected size of the sulfuryl bond lengthening/shortening effect due to this stereoelectronic interaction. To achieve this end, ab initio molecular orbital calculations were undertaken.

Ab Initio Molecular Orbital Calculations. Previous MO Studies on Sulfates. The first MO studies on sulfuric acid were at the CNDO/2 level.[29] Conformational energies given by this low level of calculation have been queried by more recent higher level calculations.[30] A more extensive study has been made by Kal-

(21) Kaliannan, P.; Vishareshwara, S.; Rao, V. S. R. *J. Mol. Struct. THEOCHEM* **1983**, *9*, 7.
(22) Gillespie, R. J.; Robinson, E. A. *Can. J. Chem.* **1973**, *41*, 2074.
(23) Kluger, R.; Thatcher, G. R. J.; Stallings, W. C. *Can. J. Chem.* **1987**, *65*, 1838.
(24) Brunvoll, J.; Exner, I. O.; Hargittai, I. *J. Mol. Struct.* **1981**, *73*, 99.
(25) Romers, C.; Altona, C.; Buys, H. R.; Havinga, E. *Top. Stereochem.* **1965**, *4*, 1939.
(26) Cosse-Barbi, A.; Dubois, J.-E. *J. Am. Chem. Soc.* **1987**, *109*, 1503.
(27) Fuchs, B.; Schleifer, L.; Tartakovsky, E. *Nouv. J. Chim.* **1984**, *8*, 275.
(28) Gorenstein, D. G.; Findlay, J. B.; Luxon, B. A.; Kar, D. *J. Am. Chem. Soc.* **1977**, *99*, 3473.
(29) Holland, P. M.; Castelman, A. W. *Chem. Phys. Lett.* **1978**, *56*, 511.
(30) Lohr, L. L., *J. Mol. Struct. THEOCHEM* **1982**, *87*, 221.

iannan and co-workers, who have determined the potential energy surfaces for rotation about the S–O bonds of H_2SO_4 and $(CH_3O)_2SO_2$ at the STO-3G level[21] (and repeated a limited number of calculations at the 4-31G level).

In the earlier ab initio study no geometry optimization was attempted.[30] A more recent study employs a geometry for dimethyl sulfate obtained from electron diffraction studies and extends these geometrical parameters to approximate the structure of H_2SO_4.[21] Very limited geometry optimization is performed at the minimal STO-3G level. Bond lengths are not geometry optimized. Despite the limitations of the minimal basis sets employed, the derived energy surfaces for H_2SO_4 and dimethyl sulfate do give general support to the presence of an anomeric effect in sulfuric acid and organic sulfates.[21] The large calculated variation in O—S—O and O=S=O bond angles with torsion angle $\leq 10°$ and $\leq 5°$, respectively, is also consistent with observations on other anomeric systems.[1a,d,26,27,31]

Choice of Basis Set and Method. The large majority of ab initio calculations on sulfates and phosphates have been carried out with an STO-3G minimal basis set. Collins et al. have compared the geometries and energies obtained by calculations at the STO-3G, 4-31G, and STO-3G* levels with experimentally derived values for a range of molecules.[19c] In a later study, three higher level basis sets are compared: 3-21G, 6-31G*, and 3-21G(*).[19a] 6-31G* is too large for use with all but the smallest of molecules. However, the 3-21G(*) basis set, which contains d-functions for second row elements only, consistently yields molecular properties uniformly close to those obtained with the larger 6-31G* basis set. From calculations on a range of species, including $(CH_3)_2SO$, SO_3 and $(CH_3)_2SO_2$, it is concluded that d-functions are essential for accurate representation of hypervalent species involving second row elements.

Our results confirm these analyses. As regards geometrical parameters, the STO-3G* basis set gives a good representation of H_2SO_4 and sulfate diesters when compared with experimental values. Furthermore, the agreement between parameters calculated at the 3-21G(*) level and experimental values is excellent. Basis sets without d-functions do not perform well in this regard.

Bond Lengths of Cyclic Sulfates. Bond lengths for +sc,–sc conformers (60°,–60°), which structurally mimic the cyclic sulfates **2** and **3**, invariably show the axial S=O bond to be longer than the equatorial S=O bond. At the STO-3G* level, this difference is between 0.008 and 0.009 Å. However, the best representation of geometry is given at the 3-21G(*) level, at which the bond length difference is calculated as 0.013 Å. Though larger, this value is still compatible with the X-ray structural data obtained for sulfates **2** and **3**, which does not reliably measure a difference in bond lengths <0.014 Å. This result suggests that the generalized anomeric effect may be responsible for the observed FTIR phenomena but that standard X-ray crystallography is not sufficiently sensitive to measure it. This does not represent proof of the presence of an anomeric effect. This must be sought by more detailed study of the influence of conformation on energy and electron distribution.

Conformational Energy Surface. Interpretation of the conformational energy surface in terms of stereoelectronic effects is complicated by the influence of steric interactions. The sp,sp conformation (0°,0°) is significantly destabilized by the steric repulsion between the two hydrogen atoms, which are held in close proximity to each other. However, on the basis of steric interactions alone, the ap,ap conformer would be predicted to be of low energy. This is clearly not the case. In fact the $\phi = 180°$ cross-section represents a line of saddlepoints and local maxima. Clearly other interactions must be operating in this system.

The anomeric effect is discussed in terms of stabilizing app interactions between polar bonds and heteroatom lone pairs, considered as sp^3 hybrids.[1a,b] The lone pairs on the bridging oxygens of H_2SO_4 may be orientated app to either S=O bond or to the adjacent S—O bond. In the latter case "cross-hyperconjugative" effects may occur.[27,32]

(31) Reference 21 and references cited therein.

Chart III

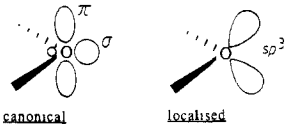

The global and local minima at the STO-3G* level are the +sc,+sc (90°,90° or 83°,83° when fully optimized) and +sc,–sc (90°,–90°) conformers, respectively. Optimal app overlap of sp^3 hybridized nonbonding electrons is predicted for the +sc,+sc (60°,60°) and +sc,–sc (60°,–60°) conformations, which are expected to possess less torsional strain. The observation of significant distortion from this predicted ideal geometry, in the observed energy minima, indicates a flaw in the "sp^3 lone pair" anomeric interpretation.

If we postulate a stabilizing stereoelectronic interaction between the nonbonding electrons of a bridging oxygen and an S=O double bond when two lone pairs on one oxygen atom are anticlinal to that double bond, optimal overlap would occur for +ac,+ac (120°,120°) and +ac,–ac (120°,–120°) conformers. Thus the observed minimum energy conformations result from stereoelectronic optimization together with minimization of the steric strain inherent in eclipsed ac and –ac (120° and –120°) S–OH bonds. Similar stereoelectronic interactions with S–O single bonds may be present, but these may be hidden by steric strain in sp conformations. Thus the high energy of ap conformers is the result of the absence of any anticlinal stereoelectronic interactions. Interestingly, optimization at the 3-21G(*) level yields a global minimum energy +ac,+ac conformer (100°,100°) and a local minimum +ac,–ac conformer (115°,–115°), i.e., with torsional angles distorted further from +sc,+sc and +sc,–sc geometry toward optimal, 120°, 120° and 120°,–120° geometries. A similar "double anticlinal" interaction has been postulated to occur between lone pairs on equatorial oxygen substituents and apical phosphorus–oxygen bonds in trigonal-bipyramidal P(V) species and is regarded as at least as strong as a single app lone pair interaction.[5] No rationale is given for this effect.

The ascendancy of the kinetic anomeric effect or antiperiplanar lone pair hypothesis in organic chemistry has resulted in discussion of the anomeric effect largely in terms of sp^3 hybridized lone pair orbitals.[1] This undoubtedly facilitates the predictive application of the hypothesis, but the electron density at oxygen is not localized along the sp^3 axes but is significantly delocalized around and between them.[1a,d] Localized hybrid orbitals are formed by transformation of canonical orbitals. The origin of the anomeric effect in H_2SO_4 and sulfate esters can be seen by consideration of these orbitals. Two types of interaction are apparent, $n_\sigma \rightarrow \sigma^*$ and $n_\pi \rightarrow \sigma^*$ (Chart III), the latter being more accessible due to the higher energy of the nonbonding π electrons. The directionality of σ and π orbitals differs from sp^3 hybrids as does the conformation for optimal overlap.

We have discussed the influence of steric and stereoelectronic effects on H_2SO_4 conformational energy. A third factor must be electrostatic interactions. However, the present data do not justify speculation as to such interactions, which are not resoundingly obvious in the calculated conformational energies.

Mulliken Population Analysis and Electron Distribution. Since steric interactions are likely to have less influence on bond overlap populations and bond order than on conformational energy, analysis of sulfur–oxygen bond overlap populations provides a more sensitive indicator of stereoelectronic effects. Conformational analysis of H_2SO_4 provides the overlap population surface and cross-sections and the charge density sections illustrated in Figures 3 and 4. It is clear that electron distribution is intimately linked with torsion angle about the S–O bonds.

S=O Bond Order. Charge density at the sulfuryl oxygen is inversely related to the overlap population of the sulfuryl bond (Figure 4a,c). The conformational dependence of these parameters

(32) Schleyer, P. v. R.; Jemmis, E. D.; Spitznagel, G. W. *J. Am. Chem. Soc.* **1985**, *107*, 6393.

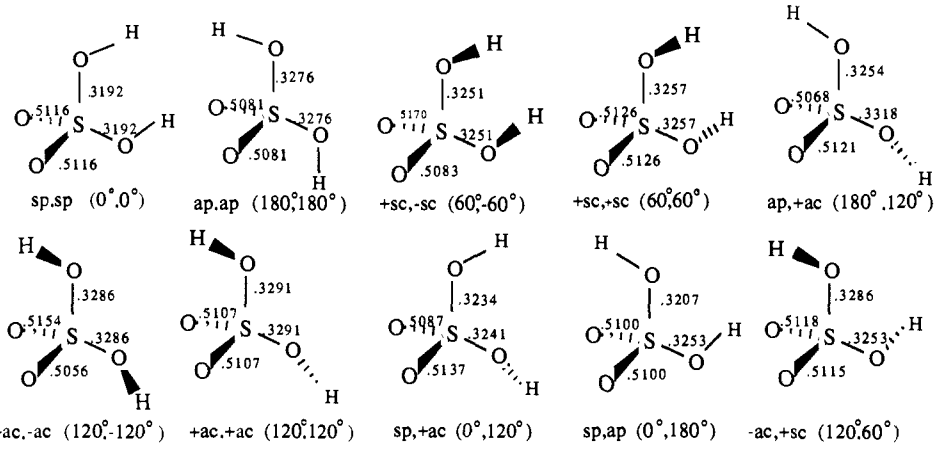

Figure 5. Sulfur–oxygen bond overlap populations (electrons) for significant conformers of H_2SO_4 from Mulliken population analysis calculated at the STO-3G(*) level. Data from Table II.

shows that when the S—O single bond has a torsional angle of 120°, a maximal shift in electron distribution occurs, from the S=O double bond to the sulfuryl oxygen. That the change in charge at the sulfuryl oxygen is almost fivefold the change in overlap population suggests the concomitant movement of electron density from sulfur into the S=O bond. The highest overlap population and minimum charge density correspond to a torsion angle of $\phi' \approx -60°$.

At $\phi' = 120°$, the sp^3 lone pairs on the oxygen are both anticlinal to the S=O bond. At $\phi' = -60°$, these lone pairs are in the opposite synclinal orientation. If these conformational trends are to be explained by an empirical stereoelectronic effect they dictate one conclusion: when the sp^3 hybridized nonbonding electrons on divalent oxygen are both orientated anticlinal to the S=O bond, this double bond is weakened and a shift in electron density occurs from this bond to the sulfuryl oxygen. This effect is minimized on rotation through 180° about the S–O single bond.

Rotation about both S–O bonds produces a cumulative effect on the S=O bond under consideration (Figure 3). A single effect is present in the +sc,+ac conformer (60°,120°), a double effect at -ac,+ac (-120°,120°), no effect at +sc,-sc (60°,-60°), and two independent effects at +sc,+sc (120°, 120°). The relative S=O bond overlap populations for these conformers are -5.5, -11.4, 0, and -6.3 me, respectively. These effects are therefore approximately additive.

S–O Bond Order. S–O single bond overlap populations show similar dependence on OS–OH torsional angle (Figure 4b). Single, zero, and two independent double anticlinal effects occur for sp,ap (0°,180°), ap,ap (180°,180°), and sp,sp (0°,0°) conformers with relative S–O bond overlap populations of -6.7, 0, and -8.4 me, respectively.

It is important to record the influence of this stereoelectronic effect on the S–O single bond bearing the oxygen nonbonding electrons. A bond strengthening feature, as in the generalized anomeric effect, is apparent. The bridging oxygen nonbonding electrons of the ap,ap conformation are involved in partial interactions with the S=O double bonds. Comparison with the +ac,+ac conformer, which possesses two optimal interactions, shows the S—O bond overlap population of this conformer relative to the "zero" ap,ap conformer to be +1.0 me.

Changes in overlap population are illustrated in Figure 5. Bond strengthening/weakening effects are apparent from examination of these structures.

Theoretical Rationale. In terms of sp^3 orbital overlap interactions, there is no obvious rationale for the observation of an optimal effect occurring when a sulfur–oxygen bond is anticlinal with respect to two nonbonding electron pairs on a second oxygen atom. We must therefore abandon the sp^3 hybrid representation and revert to canonical orbitals. The conformational dependence of electron distribution is compatible with the presence of three stereoelectronic interactions: an $n_\pi \rightarrow \pi^*$ interaction between divalent oxygen nonbonding electrons and S=O double bonds; an $n_\sigma \rightarrow \sigma^*$ interaction between divalent oxygen nonbonding electrons and S=O double bonds; and an $n_\sigma \rightarrow \sigma^*$ interaction between divalent oxygen nonbonding electrons and S–O single bonds (Chart IV). This electronic description bears comparison with that for carboxylic esters.[1b]

Chart IV

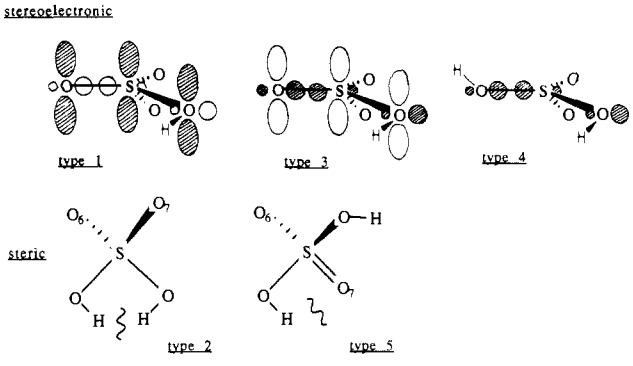

The qualitative similarity observed between the conformational energy surface calculated at the STO-3G* level (Figure 2) and that obtained at the minimal STO-3G level[21] (in the absence of d-orbital functions) provides a contra-indication for a major involvement of d-orbitals on sulfur in this bonding picture.[33]

Correlation of Conformational Energy and Electron Distribution. The conformational energy surface of H_2SO_4 is dominated by two effects: (1) a stabilizing $n_\pi \rightarrow \pi^*$(S=O) interaction; and (2) a destabilizing steric interaction between the two hydroxy hydrogens. Two further stereoelectronic interactions are apparent: (3) a stabilizing $n_\sigma \rightarrow \sigma^*$(S=O) interaction; and (4) a stabilizing $n_\sigma \rightarrow \sigma^*$(S—O) interaction. Finally, (5) a second destabilizing steric interaction is present between any hydroxy hydrogen in an eclipsed orientation with respect to a sulfur–oxygen bond Chart III.

The influence of stereoelectronic interaction (3) on the +ac,+ac (100°,100°) conformer results in this conformer being more stable than the +sc,+sc conformer (60°,60°), despite the presence in both conformers of the primary stereoelectronic effect (1). The observation that the +ac,+ac conformers are more stable than +ac,-sc and +sc,-sc conformations may be attributable to a cross-hyperconjugative effect, but it is more likely the influence of the primary steric effect (2) (or even dipole/dipole repulsion). Within this model, the relatively high energy of the ap (180°) conformers can be explained by the minimization of all three stereoelectronic interactions in this conformation.

Dimethyl Sulfate. Geometry optimization of critical conformers of dimethyl sulfate was performed at the STO-3G* level to es-

(33) In their limited early calculations, Lehn and Wipff observed that with the inclusion of d-functions, the influence of P—O torsion angles on the P=O bond overlap population was negligible.[4] However, d-orbital mixing with σ^* and π^* orbitals is not excluded (see ref 34).

(34) Wolfe, S.; Stolow, A.; La John, L. A. *Tetrahedron Lett.* **1983**, *24*, 4071.

tablish the applicability of calculations on H_2SO_4 to sulfate diesters (Table IV). Steric interactions involving the methyl groups are expected to be dominant in determining conformational energy. Nevertheless, the global minimum energy conformation is again +sc,+sc (72°,72°). Molecular models and minimal basis set ab initio calculations[21] predict that the +sc,-sc (90°,-90°) local minimum will be sterically destabilized. No minimum was located in this region. The relative energies and electron distribution of the other partially optimized conformers of dimethyl sulfate are consistent with the presence of similar stereoelectronic effects as postulated for H_2SO_4.

Acknowledgment. The authors thank the SERC for financial support. G.R.J.T. thanks the SERC for the award of a Post-doctoral Research Fellowship. The generous assistance and advice of Dr. Chris Reynolds with MO calculations is gratefully acknowledged.

Registry No. 2, 1073-05-8; **3**, 62822-77-9; **4**, 4988-33-4; H_2SO_4, 7664-93-9; 2-oxo-1,3,2-dioxathiane, 4176-55-0; 2-oxo-5-phenyl-1,3,2-dioxathiane, 62738-17-4; 1-oxothiane, 4988-34-5; pentamethylene sulfide, 1613-51-0; dimethyl sulfate, 77-78-1.

Supplementary Material Available: Tables of full geometrical parameters (bond lengths and angles), fractional atomic coordinates, and anisotropic temperature factors for compounds **2**, **3**, and **4** and full Mulliken population analysis for torsional conformation scan on H_2SO_4 (9 pages). Ordering information is given on any current masthead page.

Acidities of Glycine Schiff Bases and Alkylation of Their Conjugate Bases

Martin J. O'Donnell,*,† William D. Bennett,† William A. Bruder,† William N. Jacobsen,† Keith Knuth,† Brigitte LeClef,† Robin L. Polt,† Frederick G. Bordwell,*,‡ Susan R. Mrozack,‡ and Thomas A. Cripe‡

Contribution from the Department of Chemistry, Indiana-Purdue University at Indianapolis, Indianapolis, Indiana 46223, and the Department of Chemistry, Northwestern University, Evanston, Illinois 60201. *Received May 16, 1988*

Abstract: Equilibrium acidities in Me_2SO are reported for six ketimines of the type $Ph_2C{=}NCH(R)CO_2Et$ and five aldimines, $ArCH{=}NCH(R)CO_2Et$. Changing R in the ketimine from H to Ph increased the pK_a by 2.2 units. This surprising acidity *decrease* for Ph substitution points to a substantial increase in steric effect, as do the increases in pK_a of 3.8 and 4.2 units observed for the replacement of hydrogen by Me and $PhCH_2$, respectively. Phase-transfer alkylation of the $Ph_2C{=}NCH_2CO_2Et$ ketimine gave over 90% of monoalkylate whereas, under similar conditions, the aldimine $4\text{-}ClC_6H_4CH{=}NCH_2CO_2Et$ gave a mixture of mono- and dialkylate. The difference is that the pK_a of the monoalkylated aldimine is essentially the same as that of the parent, which leads to rapid equilibration with the parent anion and consequent dialkylation. The rates of alkylation in Me_2SO of these parent and monoalkylated anions did not differ greatly, showing that the relative pK_{HA}s of the parent acid and its monoalkyl derivative, rather than the relative rates of the mono- and dialkylation reactions, is the principal factor that determines the extent of the competition between monoalkylation and dialkylation.

Introduction

Alkylation of derivatives of the simplest amino acid, glycine, has received considerable recent attention as a preparative route to higher amino acids. The overall strategy involves removal of an α-proton from a protected glycine derivative to give an α-anion of glycine, equivalent to **1**, which is then reacted with an electrophile such as an alkyl halide to form a new carbon–carbon bond. The final step in the sequence involves removal of the protecting groups to yield the desired amino acid. Protection of a primary amino group by reaction to form a Schiff base has the added bonus of acidifying the proton alpha to the nitrogen, thereby allowing for the use of milder basic conditions to effect deprotonation. The resulting carbon–nitrogen double bond stabilized carbanion (**2**) has been used in several routes to α-substituted primary amines.[1] In conjunction with the carboxyl or equivalent protecting group it has been used extensively in the synthesis of α-amino acids.[2-10]

1 **2**

One of us has reported the phase-transfer alkylation of benzophenone Schiff base derivatives of glycine ethyl ester (**3**) and aminoacetonitrile (**4**) as a particularly attractive route to higher amino acids.[11,12] Phase-transfer alkylations are often carried out in mixtures of aqueous sodium hydroxide and a nonpolar solvent, such as PhMe or CH_2Cl_2, in the presence of a tetraalkylammonium salt. The simple reaction procedure, mild conditions,

† Indiana-Purdue University at Indianapolis.
‡ Northwestern University.

(1) (a) Bradamante, S.; Ferraccioli, R.; Pagani, G. A. *J. Chem. Soc., Perkin Trans. 1* **1987**, 515-518. (b) Mostamandi, A.; Remizova, L. A.; Pavlenkova, A. L.; Favorskaya, I. A. *J. Org. Chem. USSR (Engl. Transl.)* **1982**, *18*, 850-852. (c) Hoppe, D.; Beckmann, L. *Liebigs Ann. Chem.* **1980**, 1751-1764. (d) Asai, T.; Aoyama, T.; Shioiri, T. *Synthesis* **1980**, 811-812. (e) Arrowsmith, J. E.; Cook, M. J.; Hardstone, D. J. *J. Chem. Soc., Perkin Trans. 1* **1979**, 2364-2368 and references cited therein.

(2) Schiff base esters: (a) Duhamel, P.; Eddine, J. J.; Valnot, J.-Y. *Tetrahedron Lett.* **1987**, *28*, 3801-3804. (b) Mkairi, A.; Hamelin, J. *Tetrahedron Lett.* **1987**, *28*, 1397-1400. (c)Schöllkopf, U.; Tölle, R.; Egert, E.; Nieger, M. *Liebigs Ann. Chem.* **1987**, 399-405. (d) Genet, J. P.; Ferroud, D.; Juge, S.; Montes, J. R. *Tetrahedron Lett.* **1986**, *27*, 4573-4576. (e) Calmes, M.; Daunis, J.; Jacquier, R.; Nkusi, G.; Verducci, J.; Viallefont, P. *Tetrahedron Lett.* **1986**, *27*, 4303-4306. (f) Ikegami, S.; Hayama, T.; Katsuki, T.; Yamaguchi, M. *Tetrahedron Lett.* **1986**, *27*, 3403-3406. (g) Joucla, M.; El Goumzili, M.; Fouchet, B. *Tetrahedron Lett.* **1986**, *27*, 1677-1680. (h) Tsushima, T.; Kawada, K. *Tetrahedron Lett.* **1985**, *26*, 2445-2448. (i) Belokon', Y. N.; Chernoglazova, N. I.; Kochetkov, C. A.; Garbalinskaya, N. S.; Belikov, V. M. *Chem. Commun.* **1985**, 171-172. (j) Bey, P.; Ducep, J. B.; Schirlin, D. *Tetrahedron Lett.* **1984**, *25*, 5657-5660 and references cited therein.

(3) Amidine esters: (a) Kolb, M.; Barth, J. *Liebigs Ann. Chem.* **1983**, 1668-1688. (b) Fitt, J. J.; Gschwend, H. W. *J. Org. Chem.* **1977**, *42*, 2639-2641 and references cited therein.

(4) Lactim ethers: (a) Schöllkopf, U.; Hinrichs, R.; Lonsky, R. *Angew. Chem., Int. Ed. Engl.* **1987**, *26*, 143-145. (b) Subramanian, P. K.; Woodard, R. W. *J. Org. Chem.* **1987**, *52*, 15-18. (c) Holler, T. P.; Spaltenstein, A.; Turner, E.; Klevit, R. E.; Shapiro, B. M.; Hopkins, P. B. *J. Org. Chem.* **1987**, *52*, 4420-4421. (d) Schöllkopf, U. In *Organic Synthesis: An Interdisciplinary Challenge*; Streith, J., Prinzbach, H., Schill, G., Eds.; Blackwell: Oxford, 1985; pp 101-112. (e) Schöllkopf, U. *Pure Appl. Chem.* **1983**, *55*, 1799-1806. (f) Schöllkopf, U. *Top. Curr. Chem.* **1983**, *109*, 65-84 and references cited therein.

0002-7863/88/1510-8520$01.50/0